euspen's 24th International Conference & Exhibition, Dublin, IE, June 2024
www.euspen.eu

Calibration of reference spheres by double-ended interferometry

Tillman Neupert-Wentz[1], Guido Bartl[1], René Schödel[1]

[1]*Physikalisch-Technische Bundesanstalt*

Tillman.Neupert-Wentz@ptb.de

Abstract

Reference spheres are a standard tool for the calibration of coordinate measuring machines (CMMs). Typically, the calibration of a reference sphere considers the diameter and the sphericity on the equator. Because spheres in CMMs form the foundation of dimensional 3D metrology, it is important to develop methods that can ensure low uncertainty, easy manipulation and short calibration times with regard to other interferometric calibration techniques, for example those of the Avogadro project [1]. The required improvements are, firstly, to provide a diameter topography, and secondly, to decrease the measurement uncertainty. To fulfil these requirements, a new measurement setup has been proposed. The setup utilises PTB's double-ended interferometer (DEI) which has originally been developed for gauge block calibrations without wringing. By adding focusing optics to the measurement path, measurements on spheres can be done through interference of plane wavefronts.
In this work, the initial implementation of the proposed modifications is presented. First results are validated, and the required measurement uncertainty budget is compiled. Based on the experience of the first measurement campaign, possibilities for improvement are identified and presented.

Interferometry, reference spheres, metrology

1. Introduction

The ever-increasing industrial and scientific requirements for high-accuracy CMMs demand improvement of the calibration of such devices. A major contributor to uncertainty is the calibration of reference spheres. These spheres are used for calibrating CMM styli. To meet those demands, an extension of PTB's double-ended interferometer has been proposed [2]. This new setup aims to decrease the measurement uncertainty of calibration of reference spheres. In addition to the standard calibration data, which contains a diameter and the sphericity along the equator, this setup will provide a diameter topography. In this work, the local topography of the sphere under test (SUT) is measured. The surface covered by the local topography is defined by the system's field of view. Future work will include a positioning system to cover the whole surface of the SUT.

First the implementation of the DEI with the proposed extension is introduced. The evaluation method is presented. Then measurements on a 30 mm reference sphere are shown and discussed. A lookout on future developments is given, and the results are concluded.

2. Experimental setup

PTB's DEI, which is situated in a temperature-controlled vacuum chamber (ΔT_{24h} = ±5 mK; p = 10^{-4} hPa), consists of two Twyman-Green interferometers that share the same extended collimated light source (diameter = 80 mm). The first beam splitter divides the incident light into two partial beams, one for each interferometer (side A and B, Figure 1). Each side contains

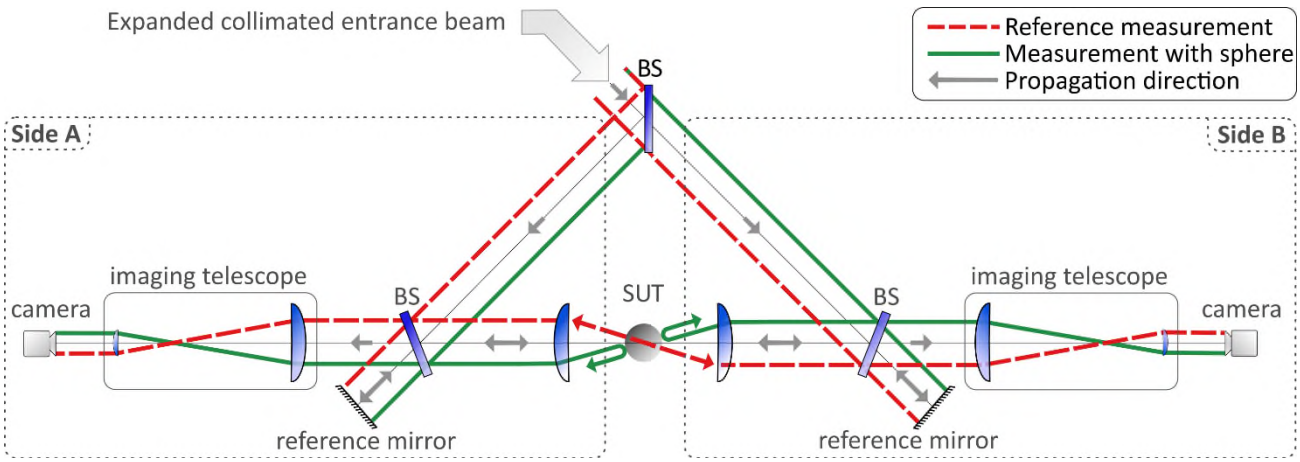

Figure 1. Setup of PTB's DEI with exemplary sections of the beam path. BS: beam splitter, SUT: sphere under test. In reference measurements the sphere is removed from the beam path.

another beam splitter which transmits the beam to the reference mirrors and reflects it towards the SUT, respectively.

Therefore, the measurement paths of each interferometer are on the same optical axis with opposite directions. Focusing optics are in front of the SUT. The centre of the SUT is placed in the coinciding focal point of these optics. Therefore, the focused beams have a right angle of incidence on the SUT. After reflection, the beam is recollimated through the optics. After superimposition with the reference beams, the interference pattern is imaged on CMOS cameras through an afocal optical system. Without the SUT in the measurement path (reference measurement, section 2.1.) this configuration yields a telescope with a magnification of 1.

Plano-aspheric lenses were chosen for this work. With a numerical aperture of 0.14 the chosen lenses provide an angular field of view of 16°. Lens topography measurements were used to select the best lenses from a batch of four. All lenses exhibit manufacturing artefacts typical for aspheric lenses. An example of such topography can be seen in [3]. The peak-to-valley value of the topography ranged from λ/6 to 2λ (at 633 nm).

For phase retrieval a five-step phase shifting algorithm is used [4]. Phase steps are introduced through piezoelectric movement of the reference mirrors.

2.1. Diameter evaluation

The evaluation method is derived in [2]. The calculation of the SUT's diameter requires two measurements: one with the SUT inside the telescope and a reference measurement with the SUT removed from the beam path. The beams then propagate through the empty telescope.

Figure 2 portrays exemplary beam paths to clarify the variables used in the equation below, which apply for the whole aperture. This set of four beam paths is necessary to calculate the diameter.

$$d_{sphere} = \frac{L_{A,ref} + L_{B,ref}}{2} - \frac{L_A + L_B}{2} \qquad (1)$$

With L the corresponding path length, index *A/B* denoting the two output sides of the interferometer and index *ref* the reference measurement without the SUT in the beam path.

To increase the unambiguity interval beyond λ/2, the coincidence criteria is applied [5]. Therefore, two iodine-stabilised lasers are used: a frequency doubled Nd:YAG laser (λ = 532 nm) and a HeNe laser (λ = 633 nm). Doing so sets the unambiguity interval to 1.6 µm.

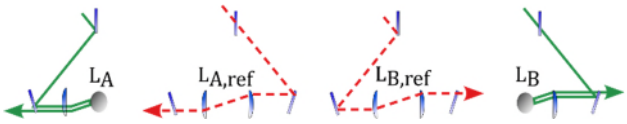

Figure 2. Path length L for sphere and reference measurement for a single diameter. Indices *A/B* correspond to the output side of the interferometer (Figure 1). Index *ref* refers to the reference measurement.

3. Measurement results

The SUT is a ceramic aluminium oxide reference sphere with a nominal diameter of 30 mm. Due to the chromatic focus shift of the lenses and a subsequent increase in uncertainty, only data for one wavelength (532 nm) will be presented.

Table 1 compares a tactile measurement of the diameter of the SUT with the result of the interferometric measurement. The tactile measurement was provided by an accredited calibration laboratory. The shown diameter obtained from the interferometric measurement is taken from the centre of the field of view of the lenses. Due to the effects described in the following paragraph, the central diameter is shown instead of the mean diameter over the field of view. The difference to the tactile measurement is 50 nm, which agrees within the measurement uncertainties.

Table 1. Comparison of SUT with tactile and interferometric measurements. The location of the measurements below, is show in Figure 4. Coverage factor k = 1.

	Value / mm	Standard uncertainty / nm
Tactile	29.99274	150
Interferometric	29.99279	190
Difference	0.00005	

Figure 3 displays the phase topographies of the measurement. Figure 4 shows the diameter topography calculated from the phase topographies in Figure 3 using Equation 1. Note that the average diameter is subtracted from the shown topography for better readability. In this topography, multiple artefacts are visible like the concentric rings that are visible at 2°, 4° and 8°. The shape of theses rings is consistent with the results of the lens topography measurements. Any aberration, including

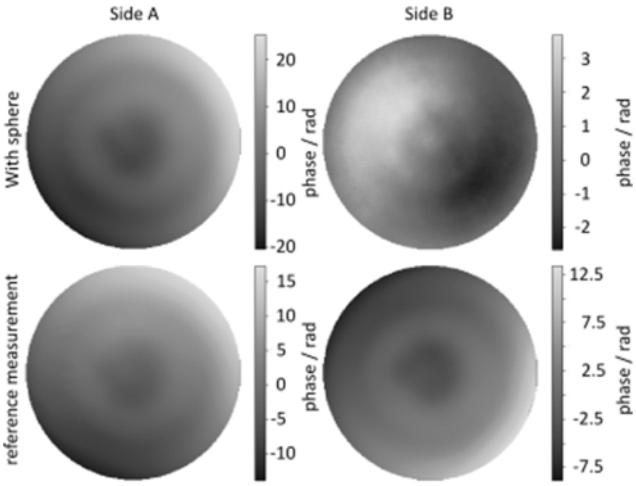

Figure 3. Phase topography of measurement with sphere and reference measurement for each interferometer side.

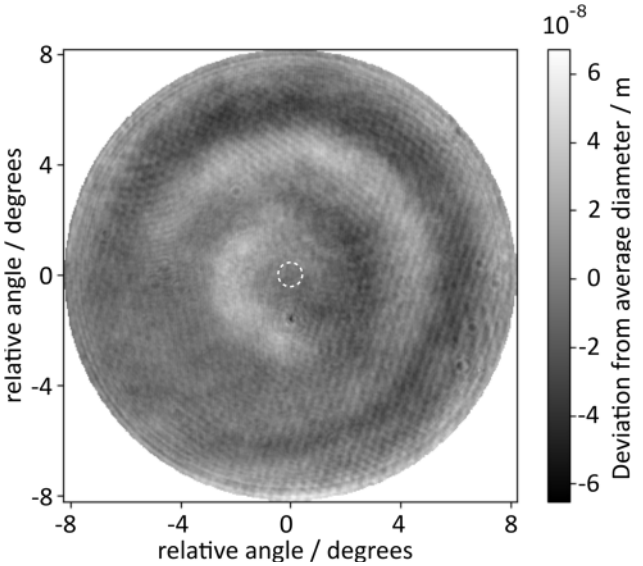

Figure 4. Deviation of the diameter topography from the average diameter within the field of view. The dashed circle marks the target position of the measurements shown in Table 1. Average diameter = 29.99309 mm.

Table 2. Major uncertainty contributions to the interferometric measurement shown in Table 1.

Contribution	Uncertainty	Sensitivity	%	Contribution
Coordinate misallocation	170 nm	1	82	170 nm
Position uncertainty	65 nm	1	11	65 nm
Parasitic reflection side A	0.66 rad	$4.24 \cdot 10^{-8}$	2.2	28 nm
Parasitic reflection side B	0.66 rad	$4.24 \cdot 10^{-8}$	2.2	28 nm
Phase change on reflection and roughness side A	40 nm	0.5	0.6	20 nm
Phase change on reflection and roughness side B	40 nm	0.5	0.6	20 nm

manufacturing artefacts, causes a misallocation of coordinates on the SUT with respect to the coordinates on the camera. This leads to a miscalculation of the diameter. The aberrations are thus transferred to the diameter topography. Furthermore, high frequency periodic structures are visible. These ripples are caused by parasitic reflection within the interferometer, i.e. between the backside of the beam splitters and the surfaces of the aspheric lenses. Every optical component within the interferometer has an anti-reflection coating with a residual reflection below 0.5 % at the relevant wavelengths. Additionally, the bulk material of the beam splitters has a 3 mrad wedge angle. Due to the interaction between two beam splitters and a reference mirror, the angle of certain parasitic reflections to the optical axis becomes zero. Therefore, some reflections from the beam splitters backside reach the camera and cause unwanted interference.

4. Uncertainty

Table 2 contains the major contributions to the measurement uncertainty of the interferometric measurement displayed in Table 1.

The largest contribution is the coordinate misallocation. This contribution is estimated through the residual aberrations after alignment. Therefore, it not only depends on the quality of the lenses but also on the alignment of the system. From the residual aberrations a maximal deviation between diametral points on the SUT is estimated. The difference between the nominal diameter and the chord that connects two deviated points amounts to the uncertainty.

Position uncertainty describes the accuracy with which the position of the measurement on the sphere can be determined. The accuracy is estimated to be ±2.5°. Within this range, the peak-to-valley value is determined which yields the uncertainty value.

Besides the parasitic reflection originating from the beam splitters as described in the previous paragraph, also, the residual reflection of the lens surfaces must be considered. Therefore, three surfaces must be considered of which the backside of the central beamsplitter and one surface of the lens are flat, and the second surface of the lens is curved. For simplicity the aspheric surface of the lens is approximated with a spherical surface that has the same focal length. The amplitude of the beam that is reflected from the curved surface is attenuated by the inverse square law. The orientation of the lenses shown in in Figure 1 indicates that the beam does not hit the flat surface of the lenses perpendicularly. Therefore, the reflected beam is divergent. To determine the influence, the amplitude of each parasitic reflection relative to the amplitude of reference and measurement beam must be evaluated. The relative intensity is determined through the losses inside the beam path and residual reflection of the anti-reflection coatings. The parasitic reflection effects the measurement for both sides of the interferometer independently, hence it must be considered twice.

Phase change in reflection and roughness is a well-known source of uncertainty of double-ended-interferometers in absolute length measurements [6]. The phase change in reflection deviates from 180° for non-dielectric materials. This moves the apparent plane of reflection away from the plane of mechanical contact depending on the complex index of refraction. Similarly, the apparent plane of reflection is moved through surface roughness. The rougher a surface, the deeper light can penetrate the SUT's surface. Hence the interferometric length will appear smaller than the mechanical length. Since no calibration method for phase change and roughness is available, literature values for ceramic gauge blocks where used [7,8]. This can only be a rough estimation but since the contribution is rather small (<1%) even being off by a factor of two, does not affect the result notably. Therefore, this estimation is deemed acceptable as long as other contributions retain their dominant influence. The approximation must be revised when the contribution of the coordinate misallocation is reduced. This effect also occurs on both sides of the SUT, therefore it also has to be considered twice.

5. Conclusion

The measurement setup proposed in [1] has been implemented. These first measurements agree with the calibration diameter within the measurement uncertainty. Although the uncertainty of the new method is still larger than that of the (tactile) calibration, these measurements can be used to identify opportunities for further improvement.

First the sensitivity to manufacturing artefacts or for that purpose all aberrations and their transmission behaviour to the diameter topography are visible. Whilst the lenses used are already the highest quality, that is available off-the-shelf, the topography measurements have shown that there is a wide range of quality. Subsequently a reduction of the influence of manufacturing artefacts can be achieved by sourcing more lenses and picking the best ones.

The influence of the parasitic reflections can be addressed through a reconfiguration of the setup. Instead of using lenses, which always have surfaces that cause parasitic reflections, off-axis-parabolic mirrors could be utilised. This would not only reduce the number of pass-through optical surfaces to zero but also eliminate any chromatic effects within the optical setup.

At last, a positioning unit will be developed that will enable the sphere to be rotated in both axes to be able to measure a full surface topography.

Acknowledgement

The authors would like to thank Eva Kuhn and Arnold Nicolaus for the fruitful discussions. Furthermore, we would like to thank Patrik Knigge for the design and construction of various mechanical components used in this work. At last, we thank Michael Neugebauer who kindly provided the reference sphere used in the experiment.

References

[1] Bartl G, Bettin H, Krystek M, Mai T, Nicolaus A, Peter A 2011 Volume determination of the Avogadro sphere of highly enriched 28Si with a spherical Fizeau interferometer *Metrologia* **48** 96-103

[2] Schödel R and Fischedick M 2021 Proposed extension of double-ended gauge block interferometers for measuring spheres *Meas. Sci. Technol.* **32** 084010

[3] El-Hayek N, Nouira H, Answer N, Damak M, Gibaru O 2014 Comparison of Tactile and Chromatic Confocal Measurements of Aspherical Lenses for Form Metrology *Intern. Journ. Of Prec. Eng. And Manufac.* **15** 821-829

[4] Tang S 1996 *Self-calibrating five-frame algorithm for phase-shifting Proc. SPIE* **2860** 91-98

[5] Schödel R 2015 Utilization of coincidence criteria in absolute length measurements by optical interferometry in vacuum and air *Meas. Sci. Technol.* **26** 084007

[6] Fichedick M, Stavridis M, Bartl G, Elster C 2021 Investigation of the uncertainty contributions of the alignment of PTB's double-ended interferometer by virtual experiments *Metrologia* **58** 064001

[7] Shutoh S, Moriyama H, Sawabe M 1998 Phase shift on ceramic gauge blocks *SPIE* **3477** 181-186

[8] Balling P, Ramotowski Z, Szumski R, Lassila A, Křen P, Mašika P 2019 Linking the optical and the mechanical measurements of dimension by a Newton's rings method *Metrologia* **56** 025008